Intermetallics 23 (2012) 32–38

Contents lists available at SciVerse ScienceDirect

Intermetallics

journal homepage: www.elsevier.com/locate/intermet

3-D morphology and growth mechanism of primary Al_6Mn intermetallic compound in directionally solidified Al-3at.%Mn alloy

Huijun Kang, Xinzhong Li*, Yanqing Su, Dongmei Liu, Jingjie Guo, Hengzhi Fu

School of Materials Science and Engineering, Harbin Institute of Technology, No. 92, West-Dazhi Street, Heilongjiang, Harbin 150001, China

ARTICLE INFO

Article history:
Received 7 November 2011
Received in revised form
12 December 2011
Accepted 21 December 2011
Available online 11 January 2012

Keywords:
A. Intermetallics, miscellaneous
C. Crystal growth
D. Microstructure

ABSTRACT

3-D morphology and growth mechanism of primary Al_6Mn intermetallic compound have been investigated in directionally solidified Al-3at.%Mn alloy at a low growth rate of 1 μm/s. A faceted growth of primary Al_6Mn with strong anisotropy has been observed. Its 3-D morphology exhibits elongated, hollow and distorted polyhedron with concave surfaces. This mainly depends on the crystal structure and growth conditions. Al_6Mn crystals tend to form regular octahedron bounded by eight {110} planes according to the crystal structure. The nonuniform transport of heat and solute during directional solidification increases the disparity in growth rates of crystal planes and strengthens the growth anisotropy. The growth of primary Al_6Mn is controlled by a screw-dislocation mechanism and terminates when nucleation of a new crystal occurs which is preferential on the concave surface. The discontinuous growth and nucleation of Al_6Mn crystal lead to a final stacking structure.

1. Introduction

Intermetallic compound has been widely introduced in alloys as a reinforced phase due to its high strength, high hardness and enhanced heat stability. In the solidification process of many commercially known cast alloys such as aluminum and magnesium alloys, a series of intermetallic compounds precipitates from the melt as primary phase, such as Al_3Ni [1,2], Al_2Cu [3,4], Al_6Mn [5,6], Mg_2Si [7,8], $Mg_{17}Al_{12}$ [9,10], etc. The size, morphology, distribution and volume fraction of these intermetallic compounds affect the mechanical properties of materials significantly. In general, fine particles or fibers of intermetallic compounds with an appropriate quantity are expected to be uniformly distributed in the matrix of solid solution for a high combination performance of materials. However, the intermetallic compound exhibiting complex crystal structures and directional bonding usually shows a faceted growth pattern with strong anisotropy and forms crystals having a wide range of morphologies and coarse sizes during solidification. For example, primary Mg_2Si intermetallic compound during solidification in Al–Mg_2Si alloys usually displays various geometric morphologies under different growth conditions, such as faceted octahedron, hopper, truncated octahedron, cube, and even non-faceted dendrite [8,11]. The inappropriate morphology and size of intermetallic compound will destroy the integrity of the matrix of solid solution and deteriorate the mechanical properties of materials. In fact, the growth morphologies of crystals mainly depend on the inherent crystal structure (determining the relative growth rates of different crystal faces) and external growth conditions (heat and solute flux, etc.). Changes of growth behavior of crystals precipitating from melt have been obtained in practice by changing the relative growth rates of different crystal planes. An example of more practical importance is that of cast iron. The addition of sulfur leads to the appearance of flake graphite while the addition of magnesium or cerium results in the formation of nodular cast iron [12].

Al_6Mn intermetallic compound with a specific stoichiometry has been determined as the most Al-rich intermetallic compound in the Al–Mn system [13,14]. Much research has focused on the precipitation processes of Al_6Mn in Al–Mn system during heat treatment [15–18]. The fine and dispersed Al_6Mn-type intermetallic compounds have been found to be precipitated from Al-matrix after heat treatment, which can effectively improve the recrystallization temperature [19], mechanical properties [20,21] and corrosion resistance [22]. Various orientation relationships between Al_6Mn and the Al-matrix were also characterized [15–18]. The research on precipitation of Al_6Mn from melt has been mainly focused on the formation of an icosahedral quasicrystal phase during rapid solidification process of Al-rich Al–Mn alloys [23–25]. The formation of this kind of quasicrystal phase as an effective reinforcement in alloys can enhance their mechanical properties

* Corresponding author. Tel.: +86 451 86418815.
E-mail address: hitlxz@126.com (X. Li).

0966-9795/$ – see front matter © 2011 Elsevier Ltd. All rights reserved.
doi:10.1016/j.intermet.2011.12.015

significantly [26,27]. However, up to now, the detailed information about the morphology feature and growth mechanism of Al_6Mn precipitated from the melt remains little.

In this paper, a Bridgman-type directional solidification experiment was conducted for Al-3at.%Mn alloy. A low growth rate of 1 μm/s was chosen to reveal morphology and growth mechanism of primary Al_6Mn intermetallic compound on the condition of nearly equilibrium solidification. A deep etched technology was used to reveal the 3-D morphology features of Al_6Mn and its growth behavior was characterized by combining the inherent growth character determined by crystal structure with the external growth conditions.

2. Preparation and characterization of samples

Al-3at.%Mn master ingot was prepared by induction melting Aluminum (99.9 wt.%) and Manganese (99.9 wt.%) under an argon atmosphere. The as-cast specimen with size of 3 mm diameter and 110 mm length was obtained from the ingot by electrical discharge machining. Directional solidification experiment was carried out in a Bridgman-type furnace. The specimen was placed into a high purity alumina tube, which was connected with a motor. The specimen was heated to 1223 K and thermally stabilized for 30 min, and then was pulled at a selected growth rate ($v = 1$ μm/s). After a growth distance of 30 mm, the specimen was quenched into the Ga–In–Sn liquid alloy to preserve the solid–liquid interface. Temperature profiles were measured separately using a PtRh30-PtRh6 thermocouple inserted within a fine alumina tube (0.6 mm internal diameter) down to the center of the samples. During the pulling process, the thermocouple moved downwards with the sample at the same pulling rate. The value of the temperature gradient can be calculated from the measured temperature profiles. The measured temperature gradient was about 25 K/mm.

The longitudinal section of directional solidification specimen was cut, followed by a standard mechanical metallographic procedure (grinding and polishing). The microstructure of specimen was characterized by scanning electron microscope (SEM-HITACHI S4700). Primary Al_6Mn intermetallic compound and its structure were identified using transmission electron microscopy (TEM-TECNAI F30). The preferred orientations of Al-matrix and Al_6Mn intermetallic compound were determined by electron backscatter diffraction (EBSD) equipment attached to SEM and rolling direction (RD) was chosen as a growth direction. EBSD data was analyzed using TSL software. A NaOH aqueous solution was used as etchant to reveal the 3-D morphology of Al_6Mn crystal which was characterized by SEM backscattered electron imagining (BSE).

3. Results and discussion

3.1. Microstructures in directionally solidified Al-3at.%Mn alloy

The relevant part of Al–Mn binary phase diagram [14] indicates that the equilibrium solidification process of Al-3at.%Mn alloy should start with a precipitation of primary Al_6Mn intermetallic compound, namely $L \rightarrow Al_6Mn$, followed by eutectic reaction $L \rightarrow Al + Al_6Mn$ at ~658 °C. With the temperature further decreases, a peritectoid reaction $Al + Al_6Mn \rightarrow Al_{12}Mn$ should occur finally at ~507 °C. In present experiment, the peritectoid reaction was not found to occur according to the characterized microstructures in TEM and SEM results. The final microstructure of Al-3at.%Mn alloy is composed of the primary Al_6Mn and eutectic ($Al + Al_6Mn$).

Fig. 1 shows SEM and TEM images of directionally solidified Al-3at.%Mn alloy at the growth rate of 1 μm/s. As shown in Fig. 1(a)–(c), the white region with long lath-like shape is primary Al_6Mn. The black region is ($Al + Al_6Mn$) an eutectic colony. The TEM image in Fig. 1(d) demonstrates that the microstructure is only composed of Al_6Mn intermetallic compound and Al-matrix phase, and the Al_6Mn with orthorhombic structure shows a typical twofold symmetry pattern as shown in Fig. 1(e). It is interesting to note that the interface between Al_6Mn and Al-matrix is sharp, and there is no obvious diffusion layer in Fig. 1(d). The primary Al_6Mn exhibits a coarse, elongated and lath-like morphology whose growth direction is basically parallel to the direction of heat flow, as shown in Fig. 1(a). A faceted growth of Al_6Mn crystal with planar and angular interfaces can be observed clearly, as shown in Fig. 1(b) and (c). Furthermore, the crystal tends to be split during growth, which causes a hollow structure. In order to reveal more details about the morphological feature, 3-D patterns of Al_6Mn crystal in directional solidification should be investigated further.

3.2. Three-dimensional morphology of Al_6Mn

A deep etching technology is used to reveal the 3-D morphology of Al_6Mn intermetallic compound by eliminating eutectic matrix, as shown in Fig. 2. Five different morphologies are frequently observed in specimens, namely cuboid (Fig. 2a), irregular octahedrons (Fig. 2b and c), hollow hopper (Fig. 2d), truncated bipyramid (Fig. 2e) and bipyramid (Fig. 2f). It is clearly shown that the shape of Al_6Mn intermetallic compound is characterized by the following aspects: faceted interface with sharp edge angles, elongated trend in growth direction, concave surfaces, and some surfaces shrinking and even degenerating into lines or points. Generally, the final shape of a crystal is mainly determined by two factors: inherent growth character determined by crystal structure and external growth conditions. The former determines the relative growth rates of various crystal planes which are significant for crystals with high entropy of fusion. The reticular density is a key factor of affecting the growth rates of planes and determining which plane is readily to remain. In addition, the orientation relationships of crystal planes also depend on the crystal structure. The latter includes solute concentration in melt, the direction of heat flow and solute rejected fields caused by competition growth between adjacent crystals, etc. All these factors affect the morphology of crystals greatly [12]. Thus, abundant morphologies of primary Al_6Mn intermetallic compound in directional solidification are observed.

3.3. Crystal structure and preferred growth direction of Al_6Mn

In order to study the effect of inherent growth character determined by crystal structure on the morphology of the primary Al_6Mn, the crystal structure and preferred growth direction of Al_6Mn should be characterized firstly. According to the classical crystallographic theory, the crystal planes with higher reticular density usually have slower growth rates, and high melting entropy increases the disparity in growth rates between low-index and high-index planes. Therefore, during the growth process, fast-growing high-index faces gradually grow out and disappear from crystals, and slow-growing low-index faces remain, leading to the formation of anisotropic morphology [12]. For example, crystals of Mg_2Si [8] with face-center cube structure and Si with diamond cube structure [28] usually show octahedral morphology bounded by eight {111} facets.

Al_6Mn intermetallic compound has an orthorhombic structure with $a = 0.75551$ nm, $b = 0.64994$ nm, $c = 0.88724$ nm [29,30], which is very complicated, as shown in Fig. 3(a). There are 28 atoms in a unit cell, including 4 manganese atoms and 24 aluminum atoms. Each manganese atom is located on the center of

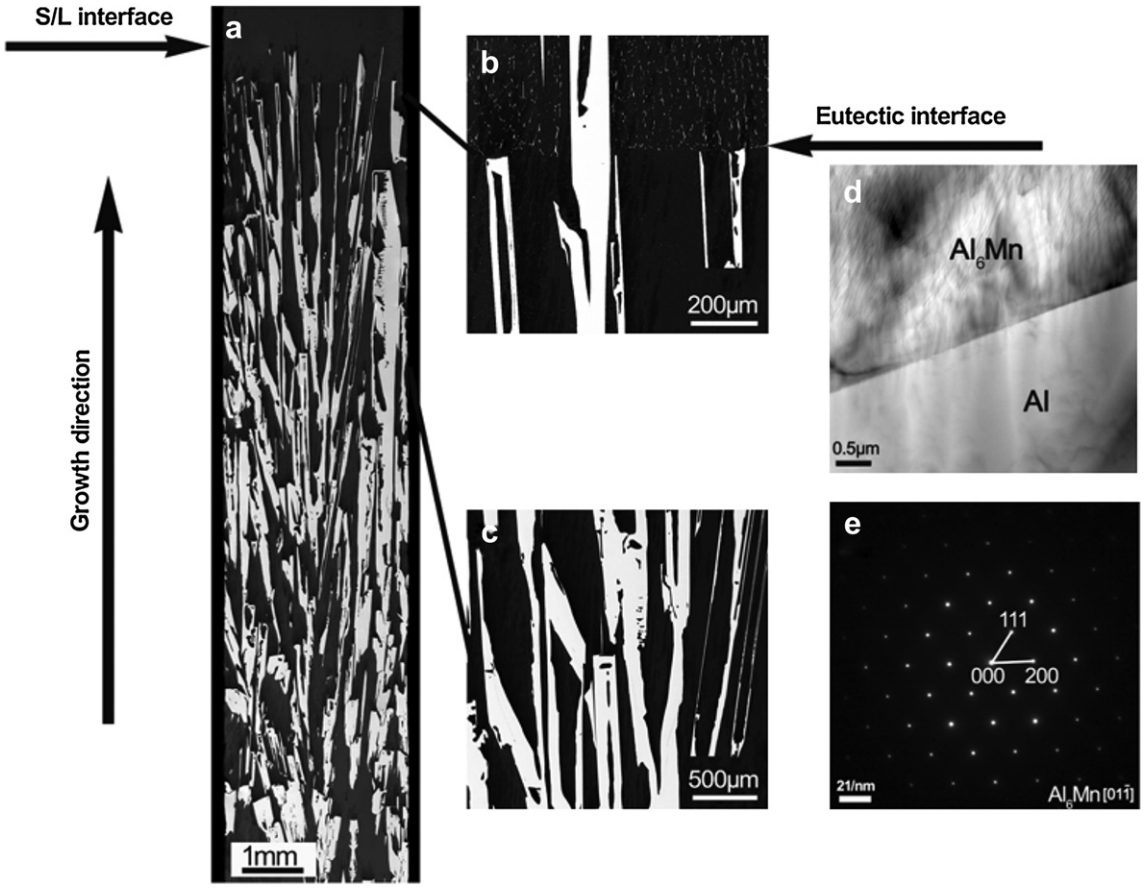

Fig. 1. Longitudinal macrostructures (a), microstructures corresponding to eutectic interface (b) and growth zone (c) in Fig. 1(a), TEM bright field image (d) and corresponding selected area electron diffraction pattern of Al_6Mn intermetallic compound (e) of Al-3at.%Mn alloy specimen directionally solidified at growth rate of 1 μm/s.

a complicated tetrakaidecahedron formed by the 10 nearest aluminum atoms, in which 8 aluminum atoms are shared by two tetrakaidecahedrons [29], as shown in Fig. 3(b). Its crystal structure is so complicated that the identification of close-packed planes of Al_6Mn is not easy. It still can be found that some closely-packed and slightly puckered layers of aluminum atoms in the Al_6Mn are parallel to the (011) and (101) planes by comparing the projections of its unit cell along the {100}, {110} and {111} directions, as shown

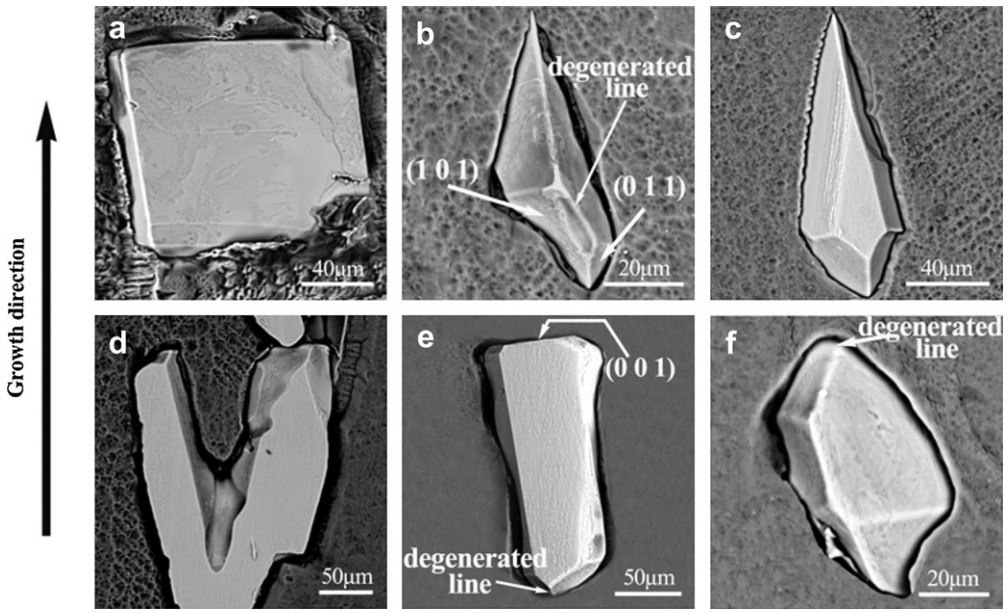

Fig. 2. Different 3-D morphologies of Al_6Mn intermetallic compound observed in directionally solidified Al-3at.%Mn alloy: (a) cuboid; (b) and (c) irregular octahedron; (d) hopper; (e) truncated bipyramid; (f) bipyramid.

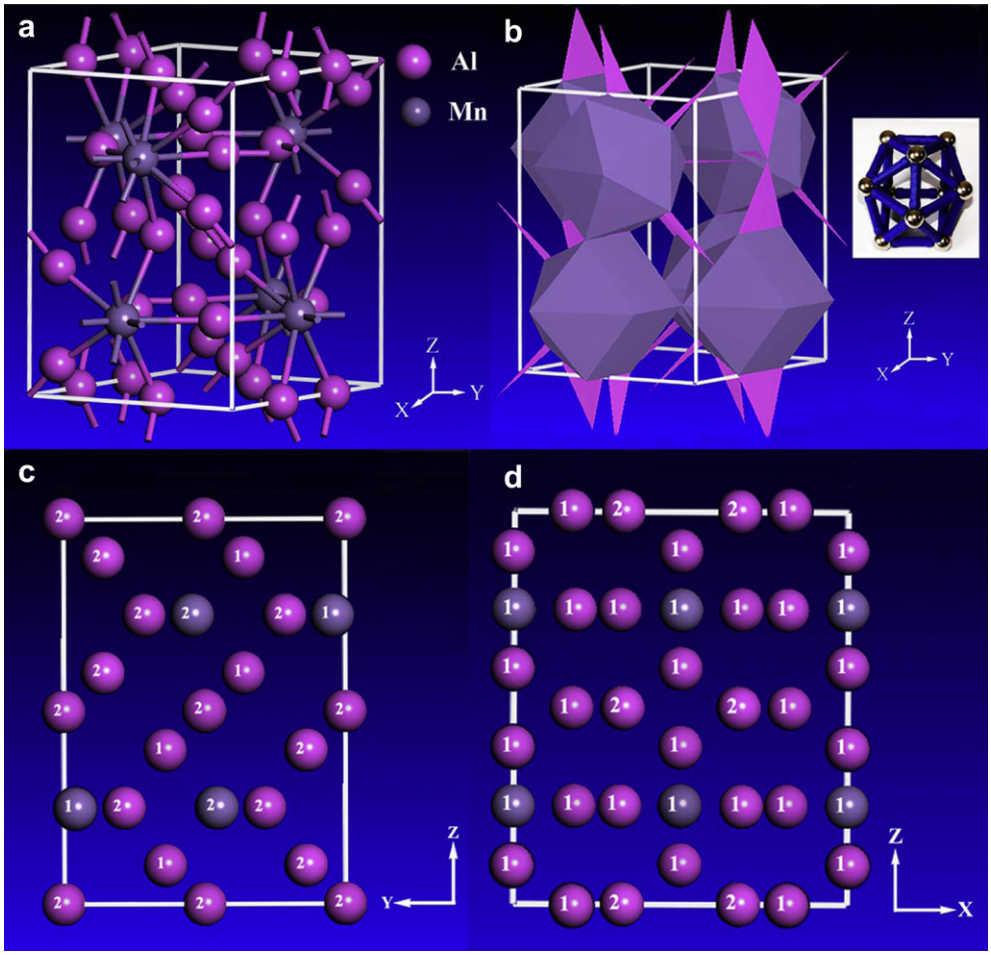

Fig. 3. The unit cell of Al_6Mn intermetallic compound (a); complicated tetrakaidecahedra composed of ten Al atoms and ball-and-stick models of the tetrakaidecahedron, steel balls represent the Al atoms and a Mn atom locates in the center of tetrakaidecahedron (b); and projections of Al_6Mn unit cell along the [100] (c) and [010] (d) directions respectively, the numbers on atoms represents the number of same kind superimposed atoms.

in the Fig. 3(c) and (d) respectively. Similar layers of atoms are also observed in other Al-rich intermetallic compounds [31]. Accordingly, the relative growth rates of (011) and (101) planes should be lower than that of other planes. It should be pointed that the definition of lattice parameters a and b in the work is opposite to Nicol's definition [29], and the positions of h and k, u and v thus should be exchanged for description corresponding to crystal orientations and planes.

Due to the effects of anisotropy of the interface energy as well as interface kinetics, the growth of crystals usually shows a preferred direction. The growth anisotropy of crystals is promoted by the preferred direction, especially in the condition of directional solidification. When the constrained growth direction of crystals is parallel to the preferred direction, most of the crystals will regularly arrange parallel to each other. Contrarily, while the constrained growth direction of crystals is unparallel to the preferred direction, crystals will grow in a radial fashion, leading to the formation of various shapes due to the competition between the constrained and preferred growth.

Therefore, it is necessary to determine the preferred growth direction of primary Al_6Mn in directional solidification, which was characterized by EBSD. Fig. 4 shows the EBSD quality map of a selected area and corresponding inverse pole figures of Al_6Mn and Al-matrix respectively. It indicates that the primary Al_6Mn and Al-matrix exhibit the preferred growth directions close to [001] and [113] respectively. The growth direction marked in Fig. 2 corresponds to the [001] crystallographic direction of Al_6Mn intermetallic compound and its Miller indexes of other directions and planes thus are deduced.

3.4. Formation of Al_6Mn

The crystal structure and EBSD results show that primary Al_6Mn crystal in directional solidification grows in preference to the [001] crystallographic direction, and tends to form octahedron shape bounded by eight close-packed (011) and (101) planes. Fig. 5 schematically shows the growth process of primary Al_6Mn crystals on the assumption that the growth is only determined by the crystal structure and the growth rates of (011) and (101) planes are consistent. Similar to cube crystal, (100), (010) and (001) planes dominate the external shape of orthorhombic crystal in the initial growth stage (Fig. 5a). As the growth proceeds, because the (101) and (011) planes with higher reticular density have lower growth rate than the (100), (010) and (001) planes, (100), (010) and (001) planes gradually shrink (Fig. 5b and c), until some {100} planes grow out and disappear (Fig. 5d). However, (101) and (011) planes remain and dominate the external shape of Al_6Mn crystal. Due to asymmetric lattice parameters ($a \neq b \neq c$) of primary Al_6Mn, the {100} planes will not disappear at the same time and some of {100} planes will degrade into a line, such as (100) and (010) planes in Fig. 5(d), which is also confirmed by the final 3-D morphology of Al_6Mn crystal in Fig. 2(b), (e) and (f). With the crystal further

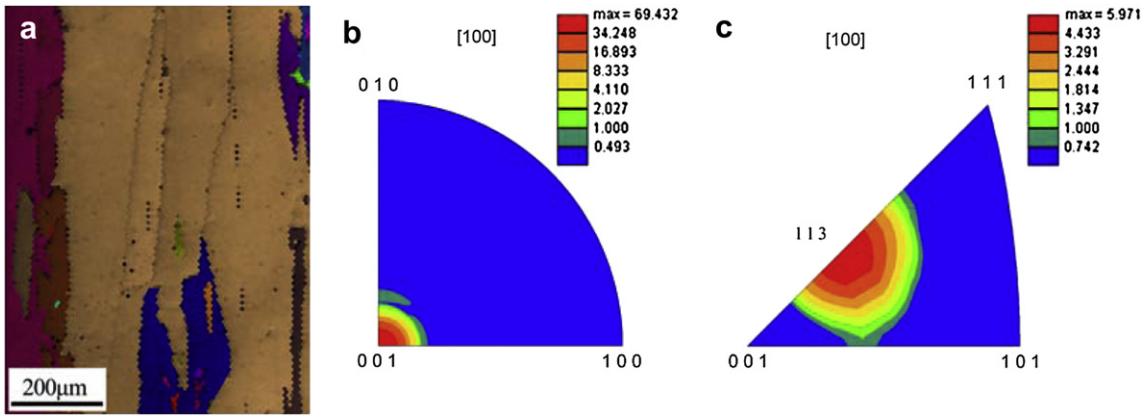

Fig. 4. EBSD image quality map of a selected area in Al-3at.%Mn alloy specimen directionally solidified at growth rate of 1 μm/s (a), corresponding inverse pole figure of Al_6Mn intermetallic compound (b) and Al phase (c).

growing, all the {100} planes disappear and change into a point. And the crystal develops into a perfect octahedron bounded by eight {110} planes. The octahedron is different from the octahedron enclosed by eight {111} planes in cube crystals. Six corners of Al_6Mn octahedron exactly match the six ⟨100⟩ crystallographic directions of Al_6Mn crystal.

In addition, it is inevitable that the crystal growth will be affected by external growth environment, especially in directional solidification process with restrictive transport of solute and heat, etc. Consequently, 3-D morphology of primary Al_6Mn in directional solidification displays an elongated, hollow and distorted polyhedron with concave surfaces, as shown in Fig. 2. The appearance of cuboid and truncated bipyramid morphologies is mainly due to the retard of growth of some {100} planes caused by the restrictive transport of solute and heat in directional solidification. In Fig. 2(a), the growth of six {100} planes is inhibited and cuboid shape visualizes, while truncated bipyramid shape in Fig. 2(e) is formed by the restraint of only two (001) planes. Additionally, impurities in the crystal will also change the growth features of some planes, and even absorb selectively on a specific plane, causing the decrease of growth rate and the changes of its morphology [32]. The emergence of {100} planes in Fig. 2(a) and (e) may also be resulted from the poisoning effect of impurities in specimens, the enrichment of impurities on some {100} planes inhibit the growth of these planes in ⟨100⟩ directions, thus {100} planes partly or completely replace {110} planes, exhibiting cuboid and truncated bipyramid shape [8,33].

Because the experiment is performed upon the condition of directional heat flow, primary Al_6Mn is elongated in direction parallel to [001] preferred growth direction. In Fig. 2(f), the 3-D bipyramid morphology of Al_6Mn is actually a typical octahedron which is stretched in preferred growth direction constrained by directional heat flow. Meanwhile, the growth rates of (011) and (101) planes close to the [001] preferred growth direction are larger than that of $(0\bar{1}1)$ and $(\bar{1}01)$ planes opposite to the preferred one. As a result, (011) and (101) planes have larger areas, as shown in

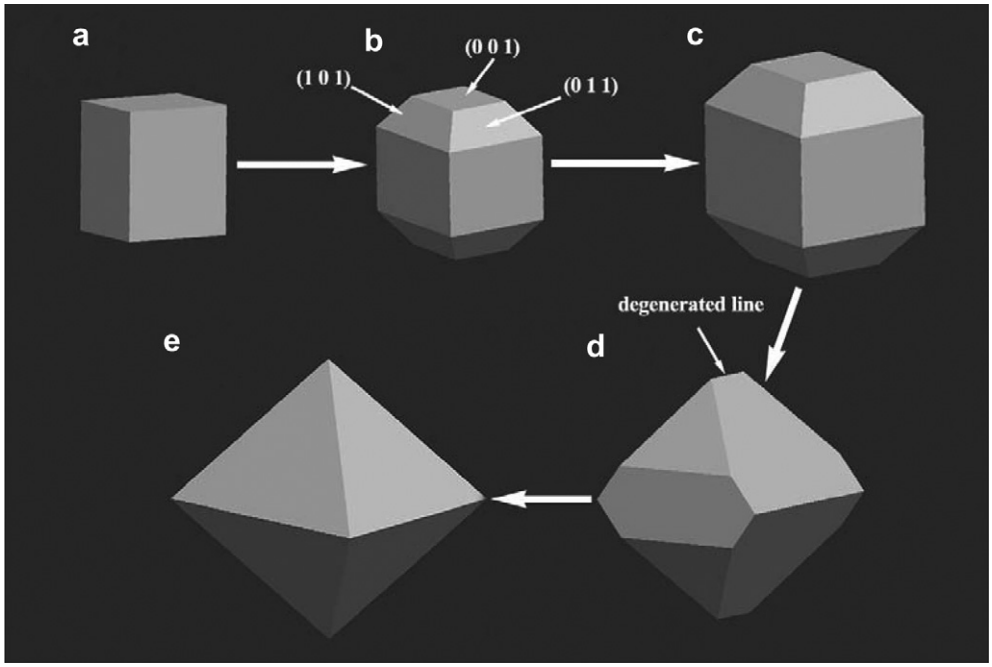

Fig. 5. A Scheme drawing of 3-D morphology evolvement of Al_6Mn intermetallic compound.

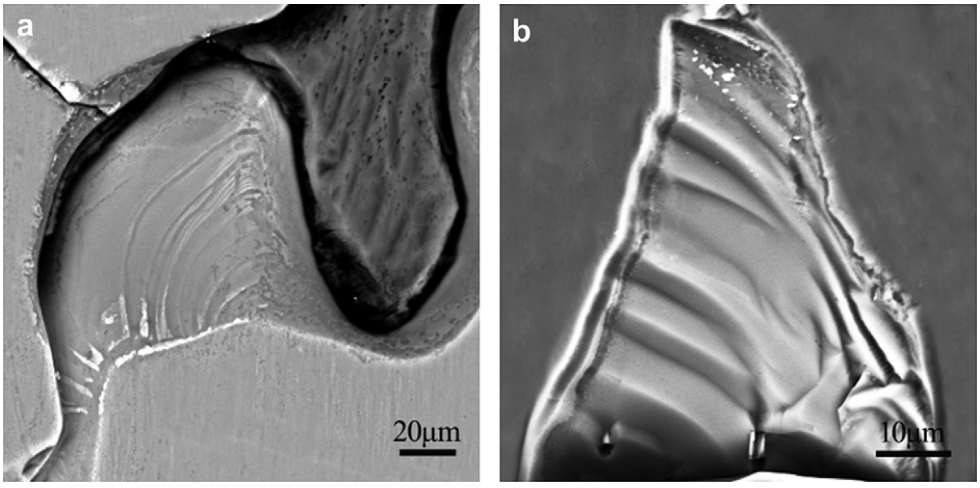

Fig. 6. Typical spiral growth steps of Al_6Mn intermetallic compound in directionally solidified Al-3at.%Mn alloy: (a) Growth traces formed by a screw-dislocation growth at the grain boundaries; (b) a greater magnification image showing clearly growth steps.

Fig. 2(b), (c) and (f). In addition, during directional growth of Al_6Mn crystals the diffusion of Al atoms into melt near the edges and corners on one surface is relatively easier than that near the center. Therefore, compared to edges and corners, the center of surface has slower growth rates [8,34], which makes the surfaces gradually concave and even forming a hollow structure inside the crystals, as shown in Fig. 2(d).

3.5. Growth mechanism of Al_6Mn

The growth of crystal with a faceted interface requires a large kinetic undercooling of the melt because of its weak trend to attach newly arriving atoms from the melt. In this case, the emergence of defects on growth interface is significant to the growth of crystals [12]. At present, two main growth mechanisms controlled by such defects are known. One is screw-dislocation controlled growth mechanism. The appearance of screw-dislocation steps on the smooth faceted interfaces will help the continuous growth of atom layers [35–37]. Another is the twin plane reentrant edge (TPRE) mechanism, in which self-perpetuating reentrant corners readily attaching atoms can be provided by two or more twins, facilitating growth of crystals in a specific direction [38]. Both the steps and reentrant corners increase the number of bonds, in which an attached atom makes with the crystal and decrease the undercooling required by the growth of crystals. Fig. 6 shows some typical spiral growth steps of Al_6Mn crystal observed in directional solidification with an average size of about 5 μm, and no TPRE growth traces are observed. The growth of primary Al_6Mn is controlled by a screw-dislocation mechanism. This growth mechanism has been widely observed during faceted growth of intermetallic compounds, such as Al_2Cu [35], Mg_2Si [35], and GaAs [37]. Weatherly [35] has evaluated the size of ledges during solid state precipitation of faceted Al_2Cu in Al–Cu alloy, which is of order of 0.04–0.05 μm. In Bauser and Strunk work [37], for GaAs grown by liquid phase epitaxy (LPE), the interstep distance of monomolecular steps is determined about 1–3 μm which is larger than that of steps. Based on the above discussion, the size of the steps may be determined by the scale atomic clusters existing in the melt and the crystal structure of the intermetallic compound. Meanwhile, the clusters can be gathered in one-, two-, or three-dimensions by vertex-linkage, or edge-, vertex-, or face-sharing polyhedra to form larger clusters [39,40]. Hence, the size of the steps should vary with types of the intermetallic compound and the growth conditions, which needs precise characterization.

As mentioned above, concave surfaces usually appear during the directional growth of Al_6Mn crystal due to the accelerated growth near the edge or corner. It leads to an abrupt depletion of solute ($k > 1$) in the melt ahead of interface and also a large undercooling which may cause a nucleation of a new crystal herein. As shown in Fig. 7(a) and (b), when the crystal shows the irregular octahedron mostly bounded by (101) and (011) planes, nucleation event is found to occur ahead of the center of the (101) or (011) concave

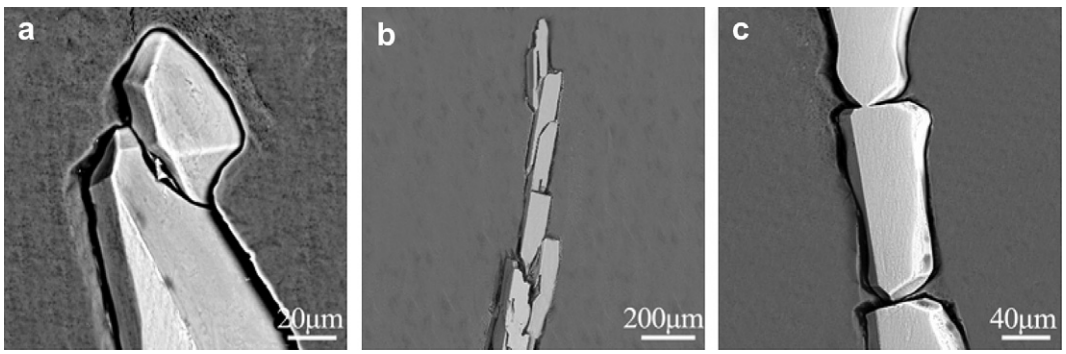

Fig. 7. Stacking growth mode of Al_6Mn intermetallic compound on different crystal planes in directionally solidified Al-3at.%Mn alloy: (a) $(\bar{1}01)$ plane; (b) (101) plane; (c) (001) plane.

surface. As mentioned above, due to the retard of growth of (001) plane, the crystal shows the truncated bipyramid. In this condition, nucleation is found to occur ahead of the center of the (001) concave surface, as shown in Fig. 7c. The nucleation of a new crystal terminates the growth of a parent crystal, and the sequent growth of the new crystal also may be terminated by a new nucleation event. By repeating in this way, a stacking structure with many Al_6Mn crystals parallel to heat flow direction is formed as shown in Fig. 1.

4. Conclusions

Deep etched 3-D morphology and growth mechanism of primary Al_6Mn intermetallic compound in directionally solidified Al-3at.%Mn alloy at a low growth rate of 1 μm/s have been investigated by combining the crystallographic analysis with effects of external growth conditions. 3-D morphology of individual primary Al_6Mn crystal is hollow, distorted polyhedron with mostly concave surfaces, and it exhibits a faceted growth pattern with a strong anisotropy. The final shape of primary Al_6Mn crystal depends on both inherent growth character determined by crystal structure and external growth conditions. The crystal structure of Al_6Mn intermetallic compound determines its regular octahedron shape bounded by eight {110} facets. The octahedron is distorted and its surfaces are concave owing to restrictive transport of solute and heat in directional solidification. The growth of primary Al_6Mn is found to be controlled by a screw-dislocation mechanism and terminates when nucleation of a new crystal which is preferential on the concave surfaces occurs. The discontinuous growth and nucleation of Al_6Mn crystal lead to a final stacking structure.

Acknowledgments

This project was supported by the National Natural Science Foundation of China (Grant nos. 51071062 and 50801019), the Foundation of State Key Lab of Advanced Metals Materials (2009ZD-06), and Project 973 (Grant no. 2011CB610406).

References

[1] Yoshimi W, Tatsuru N. Intermetallics 2001;9:33–43.
[2] Uan JY, Chen LH, Lui TS. Acta Mater 2001;49:313–20.
[3] Barbucci A, Bruzzone G, Delucchi M, Panizza M, Cerisola G. Intermetallics 2000;8:305–12.
[4] Li SM, Quan QR, Li XL, Fu HZ. J Cryst Growth 2011;314:279–84.
[5] Colinet C. Intermetallics 2003;11:1095–102.
[6] Balanetskyy S, Meisterernst G, Heggen M, Feuerbacher M. Intermetallics 2008;16:71–87.
[7] Takeuchi S, Hashimoto T, Suzuki K. Intermetallics 1996;4:S147–50.
[8] Li C, Wu YY, Li H, Liu XF. Acta Mater 2011;59:1058–67.
[9] Rosalbino F, Angelini E, Negri SD, Saccone A, Delfino S. Intermetallics 2006;14:1487–92.
[10] Kim KH, Nam ND, Kim JG, Shin KS, Jung HC. Intermetallics 2011;19:1831–8.
[11] Li C, Wu YY, Li H, Liu XF. J Alloys Compd 2009;477:212–6.
[12] Kurz W, Fisher DJ. Fundamentals of solidification. Switzerland: Trans Tech Publications Ltd.; 1998.
[13] Laissardière GT, Manh DN, Mayou D. Prog Mater Sci 2005;50:679–788.
[14] Jansson A. Metall Trans A 1992;23:2953–62.
[15] Yang P, Englerb O, Klaarc HJ. J Appl Cryst 1999;32:1105–18.
[16] Ratchev P, Verlinden B, Houtte PV. Acta Metall Mater 1995;43:621–9.
[17] Kong BO, Suk JI, Nam SW. J Mater Sci Lett 1996;15:763–6.
[18] Kong BO, Nam SW. Mater Lett 1996;28:385–91.
[19] McQueen HJ. J Met 1980;32:17–26.
[20] Park DS, Kong BO, Nam SW. Metal Trans A 1994;25:1547–50.
[21] Jo BL, Park DS, Nam SW. Metal Trans A 1996;27:490–3.
[22] Nam SW, Lee DH. Met Mater 2000;6:13–6.
[23] Schaefer RJ, Biancaniello FS, Cahn JW. Scr Metall 1986;20:1439–44.
[24] Uwe K, Bernd S. Mater Sci Eng 1988;99:417–21.
[25] Herlach DM, Gillessen F, Volkmann T, Wollgarten M, Urban K. Phys Rev B 1992;46:5203–10.
[26] Jun JH, Kim JM, Kim KT, Jung WJ. Mater Sci Eng A 2007;449–451:979–82.
[27] Schurack F, Eckert J, Schultz L. Acta Mater 2001;49:1351–61.
[28] Wang RY, Lu WH, Hogan LM. Metal Mater Trans A 1997;28A:1233–43.
[29] Nicol ADI. Acta Cryst 1953;6:285–93.
[30] Kontio A, Coppens P. Acta Cryst 1981;B37:433–5.
[31] Robinson K. Acta Cryst 1952;5:397–403.
[32] Buckley HE. Crystal growth. New York: John Wiley; 1951.
[33] Qin QD, Zhao YG, Liu C, Cong PJ, Zhou W. J Alloys Compd 2008;454:142–6.
[34] Wang RY, Lu WH, Hogan LM. J Cryst Growth 1999;207:43–54.
[35] Weatherly GC. Acta Metall 1971;19:181–92.
[36] Käss D, Strunk H. Thin Solid Films 1981;81:L101–4.
[37] Bauser E, Strunk HP. J Cryst Growth 1984;69:561–80.
[38] Hamilton DR, Seidensticker RG. J Appl Phys; 1960:1165–8.
[39] Schäfer H. J Solid State Chem 1985;57:97–111.
[40] Kim SJ, Fässler TF. J Solid State Chem 2009;182:778–89.